arXiv:1608.03674v1 [astro-ph.CO] 12 Aug 2016

The influence of host galaxy morphology on the properties of Type Ia supernovae from the JLA compilation

V. Henne[a], M. V. Pruzhinskaya[a,b,*], P. Rosnet[a], P.-F. Léget[a], E. E. O. Ishida[a], A. Ciulli[a], P. Gris[a], L.-P. Says[a], and E. Gangler[a]

[a] *Laboratoire de Physique Corpusculaire, Université Clermont Auvergne, Université Blaise Pascal, CNRS/IN2P3, Clermont-Ferrand, France*
[b] *Lomonosov Moscow State University, Sternberg Astronomical Institute, Universitetsky pr., 13, Moscow, 119234, Russia*

Abstract

The observational cosmology with distant Type Ia supernovae (SNe) as standard candles claims that the Universe is in accelerated expansion, caused by a large fraction of dark energy. In this paper we investigate the SN Ia environment, studying the impact of the nature of their host galaxies on the Hubble diagram fitting. The supernovae (192 SNe) used in the analysis were extracted from Joint-Light-curves-Analysis (JLA) compilation of high-redshift and nearby supernovae which is the best one to date. The analysis is based on the empirical fact that SN Ia luminosities depend on their light curve shapes and colors. We confirm that the stretch parameter of Type Ia supernovae is correlated with the host galaxy type. The supernovae with lower stretch are hosted mainly in elliptical and lenticular galaxies. No significant correlation between SN Ia colour and host morphology was found.

We also examine how the luminosities of SNe Ia change depending on host

*Corresponding author

Email addresses: henne-vincent@wanadoo.fr (V. Henne), pruzhinskaya@gmail.com (M. V. Pruzhinskaya), philippe.rosnet@clermont.in2p3.fr (P. Rosnet), pierre-francois.leget@clermont.in2p3.fr (P.-F. Léget), emille.ishida@clermont.in2p3.fr (E. E. O. Ishida), ciulli@clermont.in2p3.fr (A. Ciulli), philippe.gris@clermont.in2p3.fr (P. Gris), louis-pierre.says@clermont.in2p3.fr (L.-P. Says), emmanuel.gangler@clermont.in2p3.fr (and E. Gangler)

galaxy morphology after stretch and colour corrections. Our results show that in old stellar populations and low dust environments, the supernovae are slightly fainter. SNe Ia in elliptical and lenticular galaxies have a higher α (slope in luminosity-stretch) and β (slope in luminosity-colour) parameter than in spirals. However, the observed shift is at the 1-σ uncertainty level and, therefore, can not be considered as significant.

We confirm that the supernova properties depend on their environment and that the incorporation of a host galaxy term into the Hubble diagram fit is expected to be crucial for future cosmological analyses.

Keywords: Supernovae; Cosmological parameters

1. Introduction

Type Ia supernovae (SNe) are well known as cosmological distance indicators. Among the other types of supernovae they have less dispersion at maximum light and show higher optical luminosities. Through observations of distant SNe Ia the accelerating expansion of the Universe was discovered [1, 2]. The most recent analysis of SNe Ia indicates that considering a flat ΛCDM cosmology, our Universe is accelerating due to dark energy contamination ($\Omega_\Lambda = 0.705 \pm 0.034$ [3]).

However, the use of SNe Ia as "standard candles" would never be possible without the empirical relation between their peak luminosity and light curve shape. This relation was independently discovered by the American statistician and astronomer B. W. Rust and Soviet astronomer Yu. P. Pskovskii in the 1970th. Using a limited sample of Type I supernovae they were able to show that the brighter the supernova, the slower its luminosity declines after achieving maximum brightness [4, 5, 6]. Later, the dependence of colour was also reported by [7, 8].

By now several realizations of the "standardization" idea were developed: the Δm_{15}-method [9, 10], the stretch-factor [11, 2], the Multicolor Light Curve Shape (MLCS) [12, 13], PRES [14], the Spectral Adaptive Light curve Template for type Ia supernova (SALT) [15, 16], the Color-Magnitude Intercept Calibration (CMAGIC) [17]. Nevertheless, the SN Ia "standardization" procedure is one of the main sources of systematic uncertainties in the cosmological results.

The problem is that the physical properties of SN Ia explosions, which lead to the relation between SN luminosity and its light-curve shape and

colour, are still not fully understood. It is generally believed that the SN Ia phenomenon is an explosion of a CO white dwarf (WD) which exceeds the Chandrasekhar limit. However, the progenitor system is unclear. The accumulation of mass by a WD could be a result of either the matter accretion from a companion star (single degenerate mechanism, SD [18]) or merger with another WD (double degenerate mechanism, DD [19, 20]). Moreover, during the last decade the discovery of superluminous supernovae and Type Iax SNe challenges our views on possible explosion mechanisms. Without detailed spectral classification these SNe could mimic SNe Ia.

Another important factor which could violate the "standard candle" hypothesis is dust. Dust around the supernovae, as well as in the host galaxy, surely affects light curve behavior. The distribution and properties of dust in host galaxies of supernovae could be different from that in the Milky Way. Furthermore, one noteworthy ambiguity is connected to the so-called gray dust: its absorption is wavelength independent and essentially cannot be taken into account. Gray dust can be large dust particles with typical sizes greater than 0.01 μm [21]. This could lead to the dimming of distant supernovae and mimic the accelerated expansion [22]. Indeed, the amount of such dust inside host galaxies of SNe is proportional to the star formation rate, which increases into the past, and could produce an apparent fall in the luminosity of distant supernovae. However, in [23] it was shown that SNe which are free from gray dust absorption, i.e. "pure" SNe, also indicate the accelerating expansion.

At last, the metallicity of the progenitor defines the Chandrasekhar limit. A lower metallicity involves an increase of the Chandrasekhar limit and could affect the explosion process.

The above-listed factors could be considered as environmental effects. In the epoch of large transient surveys, development of observational techniques, and further processing of the data, a study of environment is of high priority.

In this paper we consider the properties of SNe and their impact on Hubble diagram in different environments. We separate Type Ia supernovae according to the type of host galaxy into three subsamples: supernovae that exploded in elliptical/lenticular (E-S0), early-type spiral (Sa-Sc), and late-type spiral (Sd-Ir) galaxies. The idea of our approach is close to the idea described in [24, 23]. The reasoning behind this idea is as follows. First, the oldest, i.e. metal-poor, stars with an age comparable to that of the Universe lie in elliptical/lenticular galaxies. This automatically leads to a more homogeneous chemical composition of the progenitor stars. Second,

the dust (including gray dust) is almost absent in these regions. And thirdly, SNe in elliptical galaxies probably have a common explosion mechanism — DD. Indeed, while in elliptical galaxies it is anyway the white dwarf merger mechanism which provides up to 99% of SN Ia explosions (see [25]), this is not the case for spiral galaxies. In the latter galaxies some fraction of SNe Ia can explode via the SD mechanism which suggests the accumulation of mass by a white dwarf from an intermediate-mass star in a binary system. The considered types of the galaxies differ in star formation rate, which is low for elliptical/lenticular galaxies and high for spirals. However, while in early-type spirals star formation regions are located in spiral arms, in late-type they are not associated with any particular structures.

Our analysis is based on the Joint Light-curve Analysis (JLA) sample of supernovae which includes 740 spectroscopically confirmed Type Ia supernovae [3]. The JLA sample is the best SNe sample to date. The main advantages of JLA compared to previous compilations are: an intercalibration between different surveys and a thorough investigation of systematic uncertainties. The presented analysis is the first study of JLA supernovae depending on host galaxy morphology.

The paper is organized as follows. In Section 2 we describe how we make a sample of SNe Ia for our analysis and how we divide them considering the morphology of the host galaxy. Section 3 contains the description of the Hubble-diagram fitting procedure. In Section 4 we perform the analysis of impact of the host morphology on SN Ia properties and compare our results with those of earlier studies. The conclusions are presented in Section 5.

2. Type Ia supernovae and host galaxy data

2.1. JLA compilation

The JLA compilation [3] regroups 740 nearby and distant supernovae up to redshift 1.3, that has been acquired between 1990 and 2008. In this sample, 374 objects come from the Sloan Digital Sky Survey (SDSS), 239 from the Supernovae Legacy Survey (SNLS), and 9 from the Hubble Space Telescope (HST). The remaining 118 are low-redshift supernovae measured by different nearby experiments. The JLA supernovae were standardized using the SALT2 model, an empirical model of spectro-photometric time evolution of SN Ia [16].

The following data for each supernova were extracted from JLA to perform the analysis:

- $z_{\rm cmb}$: the redshift in the CMB frame with its uncertainty;
- $z_{\rm hel}$: the redshift in the heliocentric frame;
- $m^*_{\rm B}$: the value of the B-band peak magnitude with its uncertainty;
- X_1: SALT2 shape parameter (stretch) with its uncertainty;
- C: SALT2 colour parameter with its uncertainty;
- ra: right ascension in degrees (J2000);
- dec: declination in degrees (J2000).

2.2. Host galaxy morphology

The morphological classification of galaxies proposed by Hubble [26, 27] and after developed by de Vaucouleurs [28] and Sandage [29] is strongly correlated with physical properties of the galaxies such as colour, mean surface brightness, neutral hydrogen content etc (see [30] for a review).

For our analysis it is important that the stellar population, amount of dust, star formation rate also evolve along the morphological sequence. Elliptical galaxies are dominated by old-stars and they are relatively dust-free. Spiral galaxies are characterized by the appearance of the spiral arms with star formation regions and diversity of stellar population. Irregular galaxies like spirals have old and young stellar populations but the star formation occurs in the absence of spiral arms [31].

Elliptical/Lenticular (E/L)						Early type spiral (ES)						Late type spiral (LS)				
cE	E	E^+	$S0^-$	$S0^0$	$S0^+$	S0/a	Sa	Sab	Sb	Sbc	Sc	Scd	Sd	Sdm	Sm	Im

Table 1: Morphological classification of galaxies implemented in the paper.

We divided the host galaxies of supernovae into three groups: elliptical/lenticular (E/L), early-type spiral (ES), and late-type spiral (LS) galaxies (see Table 1):

- E/L: in this category elliptical and lenticular galaxies were included. Elliptical galaxies have a shape of ellipse or sphere, without apparent substructure. The surface brightness is uniform in the core and declines suddenly outwards. Lenticular galaxies have a spheroidal bulge and a disk, without spiral arms.

- ES: galaxies with type from S0/a to Sc belong to the early-type spirals. This type is characterized by a prominent bulge, well formed arms and dust lanes.

- LS: the late-type spirals (Scd-Im) have loosely wound and weak arms, and a weak bulge. Both, arms and bulge completely disappear in irregular galaxies (Im) [32, 30].

Our choice was limited by statistics and difficulties connected with morphological classification. While confident detailed classification is possible only for nearby galaxies, to classify the distant galaxies usually the comparison between the observed spectra and standard spectra templates for each morphological type is applied. However, even for nearby galaxies sometimes there is a contradiction between different catalogs. For instance, the host galaxy of nearby SN 1993O in our sample is classified as S0 and Sb by different authors [33, 34].

To classify host galaxies of the SDSS supernovae we used the data provided by [35]. Zheng et al. have developed automatic classification programs to define SN and host-galaxy types as well as precise redshifts, exploring template cross-correlation and principal component analysis. The morphological types for host galaxies, independently provided by both techniques, are given in Table 3 and 4 of [35]. We made a cross-correlation between JLA SNe and Zheng et al. data; 77 coincidences were found. For 18 galaxies [35] provides several morphological types. In such case we adopted the type obtained by cross-correlation method. If cross-correlation gives several possible types we chose the one corresponding to the highest best-fit criterion.

The host morphology for nearby supernovae was extracted from different sources [33, 34, 32, 36]. If different catalogs provided the different morphological types for the same galaxy, the final decision was rendered by visual examination of images.

We did not find in the literature the detailed morphology of hosts of SNLS SNe in the JLA sample.

The classification of JLA HST supernovae can be found in [37, 38]. However, this classification divides hosts on early-type (E/S0) and late-type (S) galaxies that is not enough for our analysis.

Therefore, the detailed host classification was found for 192 SN Ia from JLA sample (see Table 2). The full list of 192 SNe is presented in Appendix (Table 6).

Host type	Number of SNe
E/L	39
ES	88
LS	65
Total:	192

Table 2: Final sample of SN Ia relative to host galaxy type. The redshift range is $0.01 < z < 0.4$ for the whole sample.

3. Hubble diagram fitting

The cosmological analysis is based on empirical relations between the light curve parameters and absolute magnitude of supernovae [8]. We use SALT2 parameters X_1 describing the time stretching of the light-curve and the colour offset with respect to the average at the date of maximum luminosity in the B-band, $C = (B-V)_{\max} - \langle B-V \rangle$.

In this analysis we adopt the classical standardization of the distance modulus:

$$\mu = m_{\rm B}^* - (M_{\rm B} - \alpha X_1 + \beta C), \tag{1}$$

where $M_{\rm B}$ is a standardized absolute magnitude of the SN Ia in the B-band for $X_1 = C = 0$, α and β describe, consequently, the stretch and colour law for the whole sample. The standardized absolute magnitude of a SN can be defined as $M = M_{\rm B} - \alpha X_1 + \beta C$. The value of the B-band apparent magnitude $m_{\rm B}^*$ at maximum light, stretch factor X_1 and colour C are taken directly from the JLA dataset [3], while the three nuisance parameters $M_{\rm B}$, α and β are free parameters of the Hubble diagram fit, as well as the cosmological parameter Ω_Λ. All free parameters are determined by minimizing the following chi-square:

$$\chi^2 = [\mu(M_{\rm B}, \alpha, \beta) - \mu_{\rm theory}(\Omega_\Lambda)]^\dagger V^{-1} [\mu(M_{\rm B}, \alpha, \beta) - \mu_{\rm theory}(\Omega_\Lambda)], \tag{2}$$

where μ is given by equation 1, $\mu_{\rm theory} = 5 \lg d_{\rm L} - 5$, where $d_{\rm L}$ is the luminosity distance in parsecs. V is a full covariance matrix of the vector of the distance modulus estimates that includes uncertainties in cosmological redshift due to peculiar velocities, the magnitude variations due to gravitational lensing, the uncounted intrinsic variation in SN magnitude, and different

systematic errors such as calibration and bias uncertainties (for the full description of the covariance matrix see [3]). The Hubble constant is fixed, $H_0 = 70$ km s^{-1} Mpc^{-1}, and the fit assumes a flat Universe dominated by its matter content $\Omega_{\rm m}$ and the dark energy Ω_Λ, i.e. such that $\Omega_{\rm m} + \Omega_\Lambda = 1$.

The fit we applied is absolutely the same as described in [3]. However, in the JLA fit one more additional parameter was introduced. It was assumed that $M_{\rm B}$ is related to the host stellar mass by a simple step function:

$$M_{\rm B} = \begin{cases} M_{\rm B} & \text{if } M_{\rm stellar} < 10^{10} M_\odot \\ M_{\rm B} + \Delta_{\rm M} & \text{otherwise.} \end{cases} \tag{3}$$

To study the environmental effects of SNe Ia we removed this correction as well as the corresponding component of the full covariance matrix from our fitting procedure.

The χ^2 has been minimized with the minimizer "iminuit" of python 2.7.

Due to the fact that we use only a part of the JLA sample (192 SNe), first, we checked that our sample is unbiased by comparing the Hubble diagram fit of the selected sample to the full JLA dataset, as shown in Table 3. The results are compatible within one standard deviation, except for the β parameter which varies up to about 2-σ. This difference can express the fact that the selected sample of SNe Ia is not fully representative of the full JLA dataset in term of colour. It could be also connected to the colour evolution with redshift [39]. One important point is that the selected sample gives a cosmological result in agreement with the full JLA dataset. To examine the systematic effects due to redshift we made the plot of the redshift distribution of the three types of galaxies (see Fig. 1, left plot). For all three subsamples the redshift is distributed in the same way.

4. The study of environmental effects

4.1. Stretch and colour

Before studying the impact of the host galaxy morphology on the Hubble diagram fitting we analyze the stretch and colour distributions for each SN subsample.

The correlation between the stretch-factor and host galaxy properties was found in previous studies [40, 7, 41, 42, 24]. It was established that the SNe Ia with the slowest decline rate, therefore, the most luminous ones, appear in galaxies with a younger stellar population (spiral and irregular galaxies).

	Full JLA sample	Our sample
Number of SNe	704	192
$z_{\max}$	1.3	0.4
χ^2/dof	0.99	0.79
Ω_Λ	0.720 ± 0.033	0.740 ± 0.088
α	0.132 ± 0.006	0.137 ± 0.011
β	3.12 ± 0.08	2.75 ± 0.15
$M_{\rm B}$	-19.08 ± 0.02	-19.11 ± 0.03

Table 3: Best-fit parameters for the full JLA dataset and the sample extracted from JLA and used in the current analysis. $\Delta_{\rm M} = 0$ in both cases.

	$\langle X_1 \rangle$	X_1 RMS	$\langle C \rangle$	C RMS
Our sample	-0.19 ± 0.08	1.07 ± 0.06	-0.009 ± 0.006	0.081 ± 0.004
E/L	-0.93 ± 0.17	1.06 ± 0.12	-0.023 ± 0.010	0.060 ± 0.007
ES	-0.18 ± 0.11	1.04 ± 0.08	-0.008 ± 0.009	0.088 ± 0.007
LS	0.25 ± 0.11	0.86 ± 0.08	-0.003 ± 0.010	0.081 ± 0.007

Table 4: The mean values and RMS for stretch X_1 and colour C for our full sample and the three subsamples.

The results of this analysis are represented in Table 4 and visualized in Fig. 2. The trend in stretch behavior is found. Low-stretch supernovae appear in E/L galaxies, the intermediate-stretch supernovae are related to ES galaxies, and the highest average stretch belongs to supernovae in LS hosts. If we assume that star formation rate connects with host galaxy morphology, so that low-star formation rate is common for elliptical galaxies, and that high-star forming regions are usually located in arms of spiral galaxies, our results are consistent with [43, 34, 44, 45, 46]. They found that low-stretch supernovae are preferentially hosted by galaxies with little or no ongoing star formation. Moreover, [44, 46] showed that fast decline rates (low-stretch) SNe Ia are almost absent in low-$M_{stellar}$ galaxies and usually happen in more massive galaxies. This result is consistent with ours, as illustrated by Fig. 1 showing that E/L hosts have the highest stellar mass, on average.

In addition, a small trend between SN colour and host galaxy type is identified. SNe Ia in E/L galaxies have slightly bluer colour than others (see Table 4). This could be explained by the fact that early-type and late-type spirals contain more dust which make the SN colour redder. However, the errors are too large to allow a conclusion.

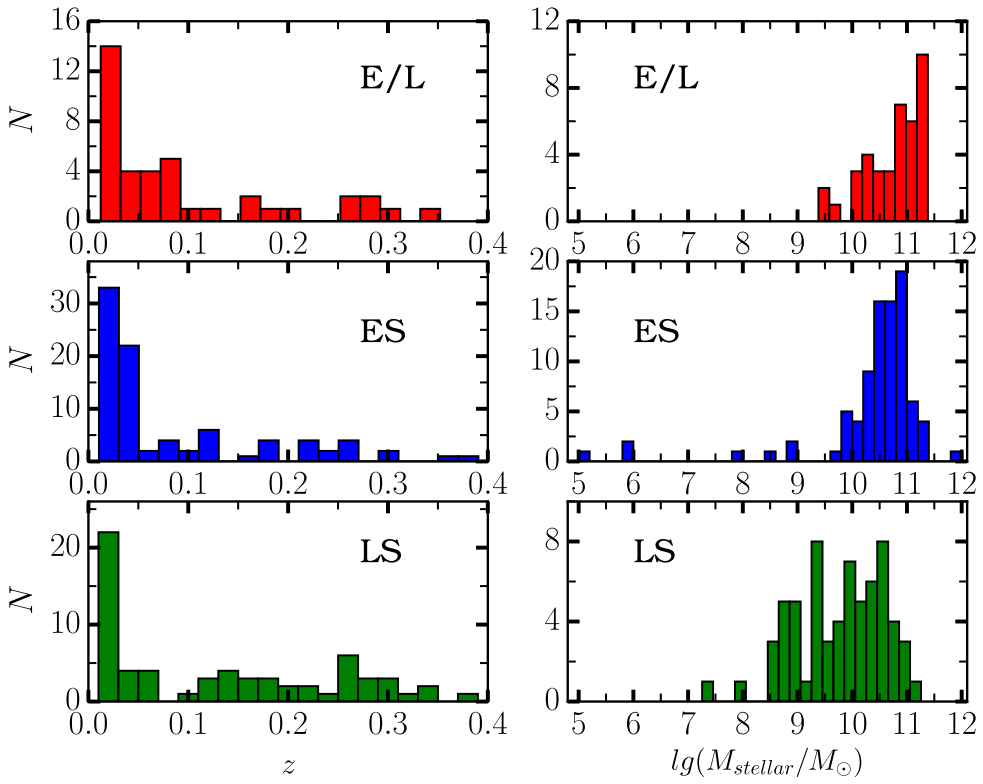

Figure 1: Redshift (left) and stellar mass (right) distributions for different host galaxy morphologies.

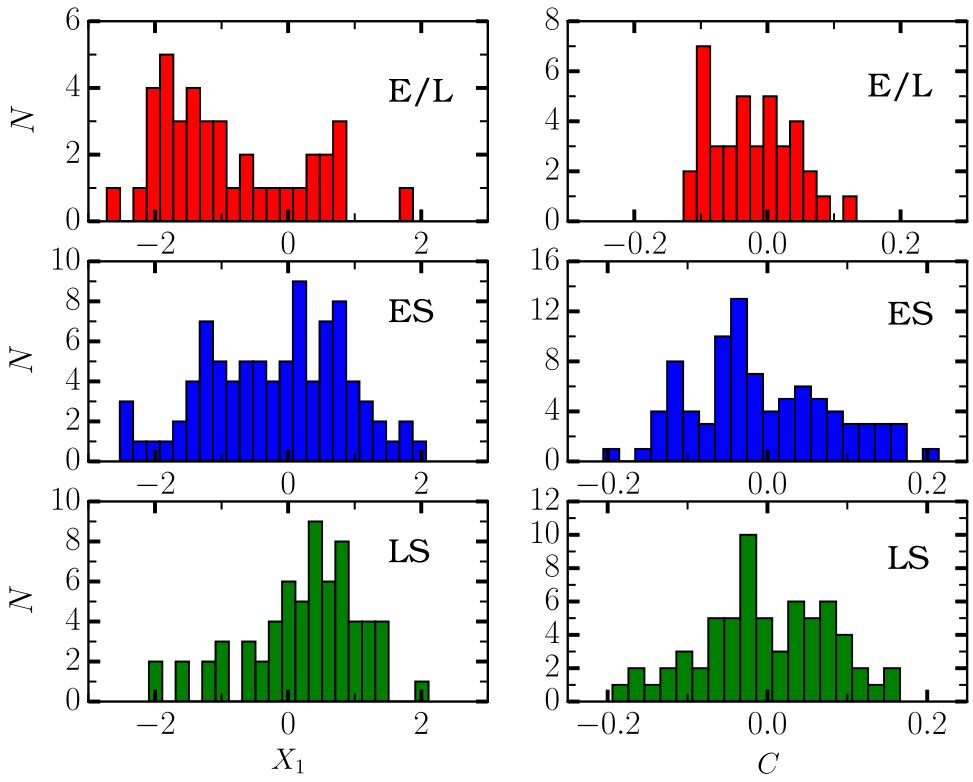

Figure 2: The distribution of the SALT2 parameters, stretch X_1 (left) and colour C (right) for different host galaxy morphologies.

4.2. Hubble residuals and RMS

We apply two different approaches. First, we examine the residuals for each subsample of SNe Ia from one global fit in which the α, β, and $M_{\rm B}$ parameters are common for the entire sample. The second approach examines the residuals and the variation of the three nuisance parameters, $M_{\rm B}$, α, and β, by performing a separate fit for each subsample (e.g., [44]). We aim to investigate if SNe Ia could be physically different in the separate samples due to environmental effects. Therefore, we assume constant cosmological parameters in both approaches ($\Omega_\Lambda = 0.705$ [3]).

The Hubble diagram for the full selected sample of 192 SNe Ia is presented in Fig. 3. The different subsamples are indicated by different colours. The average residuals $\langle\Delta\mu\rangle$ for all three types of host are compatible with zero (see Table 5). However, the RMS in E/L hosts is a bit higher than the one in LS galaxies. This result suggests that SN Ia could be different in the considered types of galaxies.

	$\langle\Delta\mu\rangle$	$\Delta\mu$ RMS	χ^2/dof	α	β	$M_{\rm B}$
Our sample	-0.011 ± 0.010	0.138 ± 0.007	0.79	0.136 ± 0.011	2.74 ± 0.14	-19.09 ± 0.02
E/L	-0.022 ± 0.023	0.144 ± 0.016	0.92	0.136	2.74	-19.09
ES	-0.004 ± 0.016	0.146 ± 0.011	0.87	0.136	2.74	-19.09
LS	-0.014 ± 0.016	0.125 ± 0.011	0.69	0.136	2.74	-19.09
E/L	-0.001 ± 0.023	0.143 ± 0.016	0.86	0.165 ± 0.025	2.75 ± 0.39	-19.14 ± 0.04
ES	-0.005 ± 0.016	0.147 ± 0.011	0.86	0.139 ± 0.016	2.91 ± 0.21	-19.09 ± 0.02
LS	-0.011 ± 0.014	0.115 ± 0.010	0.64	0.105 ± 0.023	2.50 ± 0.24	-19.10 ± 0.03

Table 5: The results of Hubble diagram fitting for the full selected sample and two approaches we used, with fixed and free α, β and $M_{\rm B}$ parameters. $\langle\Delta\mu\rangle$ is the average of the residuals. The cosmology is fixed at $\Omega_\Lambda = 0.705$.

To better understand the reason of the RMS variations we perform the Hubble diagram fitting for each subsample of supernovae separately. The fitting parameters are collected in Table 5. Fig. 4 shows the joint confidence contours in the three combinations of α, β and $M_{\rm B}$ parameters for each SN subsamples. $M_{\rm B}$ parameter is almost left unchanged under the uncertainties. The shift in the β parameter is also included in the uncertainties. On the other hand, there is a systematic shift of the value of the α parameter. Using the current values of the nuisance parameters and the average values of X_1 and C for each subsample, we calculate the average absolute magnitudes in B-band: $\langle M_{\rm E/L}\rangle = -19.05 \pm 0.11$, $\langle M_{\rm ES}\rangle = -19.09 \pm 0.05$, $\langle M_{\rm LS}\rangle =$

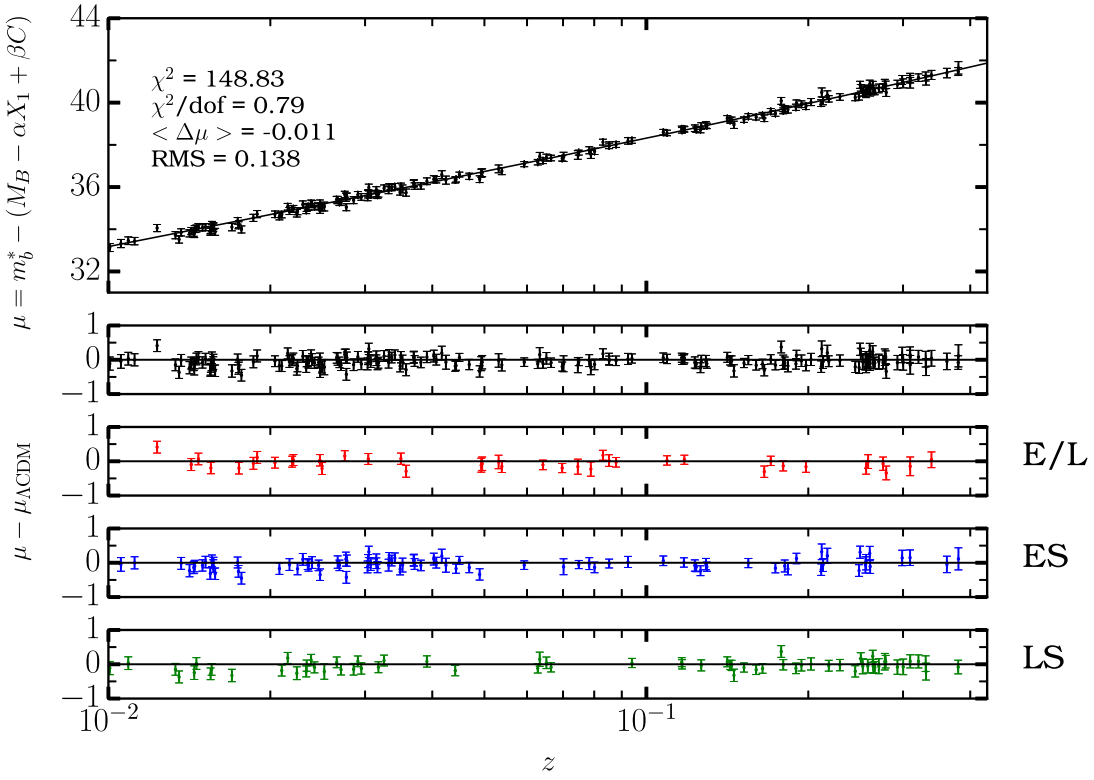

Figure 3: The Hubble diagram for the full selected sample of SN Ia (192 SNe) with identified host galaxy morphology. The residuals for the three morphological subsamples of SN Ia from one global fit in which the α, β, and $M_{\rm B}$ parameters are common for the entire sample are presented. The cosmology is fixed at $\Omega_\Lambda = 0.705$.

-19.13 ± 0.05. The obtained result does not agree with results from previous studies where after light-curve and colour corrections SN Ia are brighter in E/S0 galaxies or in low star-formation hosts than those in late-type spirals or high star-formation hosts [47, 44]. The α, β, and $M_{\rm B}$ parameters parametrize the luminosity variations within the SN Ia samples and are likely related to the physics of the SN Ia explosion and/or the SN Ia environment. Therefore, the found difference even in one parameter (α) emphasizes the importance of the environment in SN Ia studies.

SNe Ia from LS galaxies (star-forming) appear to be more homogeneous than the others. The Hubble residual dispersion is smaller for them (0.115 ± 0.010) in comparison with the full sample residual dispersion (0.138 ± 0.007). This result suggests that a division of SNe Ia by types according to the morphology of their host galaxies would improve the future cosmological analysis. Previous studies supported the idea that SNe Ia in locally star-forming regions are more appropriate for cosmology due to their low brightness dispersion [48].

5. Conclusions

We derived the host galaxy morphology for 192 SNe Ia from the nearby and SDSS JLA sample. The supernovae were divided into three subsamples depending on host morphology: elliptical/lenticular (E/L), early-type spiral (ES), and late-type spiral galaxies (LS).

Our main conclusions are:

1) As was previously shown by other studies, the SN Ia stretch parameter is closely correlated with host morphology. The low stretch (fast decline) SNe usually exploded in E/L galaxies, i.e. in old stellar population environment.

2) We did not find a statistically significant trend for the colour parameter.

3) We found a trend in the stretch nuisance parameter α. Its value decreases from E/L to LS galaxies.

4) We saw that, in an old stellar population and with low dust environment, supernovae are intrinsically fainter after stretch and colour corrections. This conclusion contradicts the results obtained by [47] (see also [44] and references in it). However, our results are consistent within 1-σ for all subsamples. This can be improved by adding SNLS JLA supernovae in the analysis.

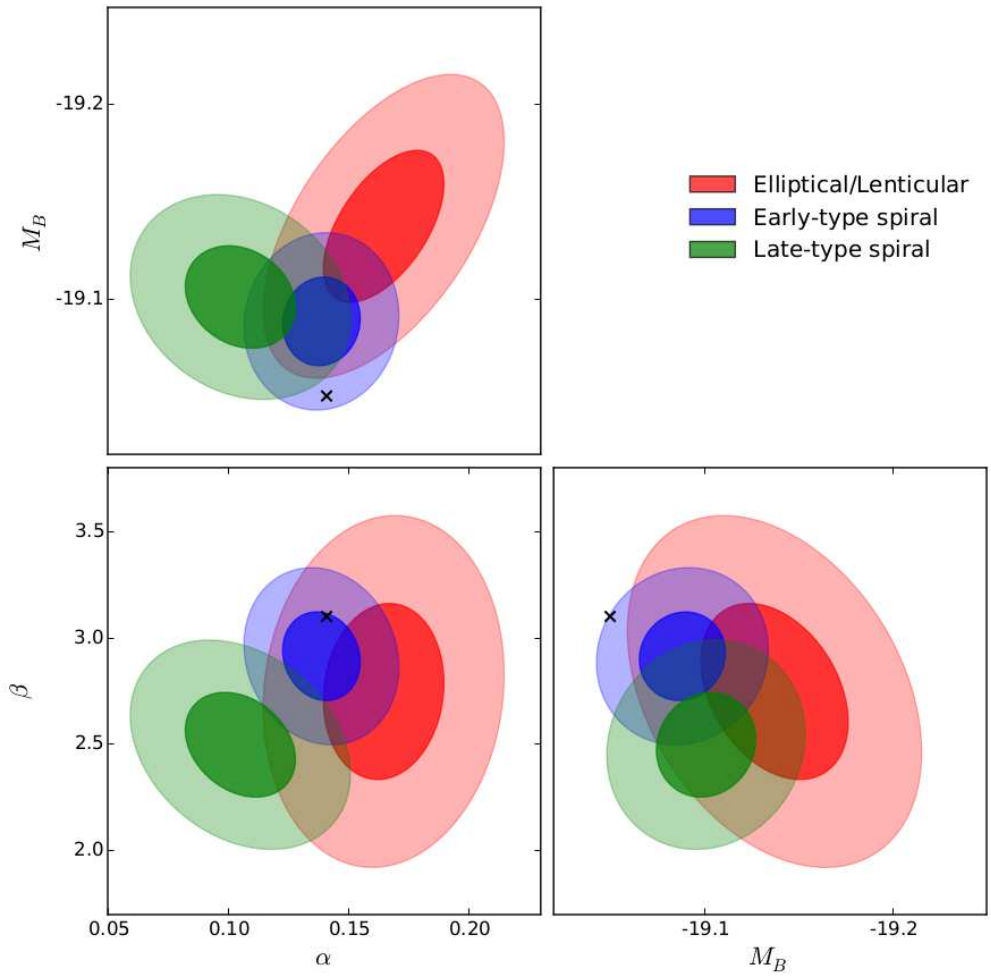

Figure 4: Joint confidence contours (1- and 2-σ) in two-parameter plots of α, β and $M_{\rm B}$ for fits where the SNe are split according to the host galaxy morphology. The black crosses represent the best fitting values ($\alpha = 0.141$, $\beta = 3.101$, $M_{\rm B} = -19.05$) from [3]. The cosmology is fixed at $\Omega_\Lambda = 0.705$.

5) The host galaxy morphology affects the residual dispersion in the Hubble diagram. We noticed that SNe Ia in LS are more homogeneous with RMS $= 0.115 \pm 0.010$.

The variation of the light curve parameters, especially the luminosity, with morphological type of host galaxy influences the cosmological analysis (e.g., [47, 48]). We conclude that for further cosmological studies the environmental effects should be taken into account.

6. Acknowledgements

The authors thank Marc Betoule for the discussion and technical issue, and acknowledge Rick Kessler, Masao Sako, and Ravi Gupta for their help with SDSS data. We thank the reviewer for his/her thorough review and highly appreciate the comments and suggestions. The authors acknowledge the Université Blaise Pascal, the French CNRS-IN2P3 agency and the Région Auvergne-Rhône-Alpes for their funding support. The work of M.V.P. (writing of the paper and comparison of the results with previously published results) was supported by RSCF grant no. 14-12-00146.

References

[1] A. G. Riess, A. V. Filippenko, P. Challis, A. Clocchiatti, A. Diercks, P. M. Garnavich, R. L. Gilliland, C. J. Hogan, S. Jha, R. P. Kirshner, B. Leibundgut, M. M. Phillips, D. Reiss, B. P. Schmidt, R. A. Schommer, R. C. Smith, J. Spyromilio, C. Stubbs, N. B. Suntzeff, and J. Tonry, "Observational Evidence from Supernovae for an Accelerating Universe and a Cosmological Constant," *AJ*, vol. 116, pp. 1009–1038, Sept. 1998.

[2] S. Perlmutter, G. Aldering, G. Goldhaber, R. A. Knop, P. Nugent, P. G. Castro, S. Deustua, S. Fabbro, A. Goobar, D. E. Groom, I. M. Hook, A. G. Kim, M. Y. Kim, J. C. Lee, N. J. Nunes, R. Pain, C. R. Pennypacker, R. Quimby, C. Lidman, R. S. Ellis, M. Irwin, R. G. McMahon, P. Ruiz-Lapuente, N. Walton, B. Schaefer, B. J. Boyle, A. V. Filippenko, T. Matheson, A. S. Fruchter, N. Panagia, H. J. M. Newberg, W. J. Couch, and T. S. C. Project, "Measurements of Ω and Λ from 42 High-Redshift Supernovae," *ApJ*, vol. 517, pp. 565–586, June 1999.

[3] M. Betoule, R. Kessler, J. Guy, J. Mosher, D. Hardin, R. Biswas, P. Astier, P. El-Hage, M. Konig, S. Kuhlmann, J. Marriner, R. Pain, N. Regnault, C. Balland, B. A. Bassett, P. J. Brown, H. Campbell, R. G. Carlberg, F. Cellier-Holzem, D. Cinabro, A. Conley, C. B. D'Andrea, D. L. DePoy, M. Doi, R. S. Ellis, S. Fabbro, A. V. Filippenko, R. J. Foley, J. A. Frieman, D. Fouchez, L. Galbany, A. Goobar, R. R. Gupta, G. J. Hill, R. Hlozek, C. J. Hogan, I. M. Hook, D. A. Howell, S. W. Jha, L. Le Guillou, G. Leloudas, C. Lidman, J. L. Marshall, A. Möller, A. M. Mourão, J. Neveu, R. Nichol, M. D. Olmstead, N. Palanque-Delabrouille, S. Perlmutter, J. L. Prieto, C. J. Pritchet, M. Richmond, A. G. Riess, V. Ruhlmann-Kleider, M. Sako, K. Schahmaneche, D. P. Schneider, M. Smith, J. Sollerman, M. Sullivan, N. A. Walton, and C. J. Wheeler, "Improved cosmological constraints from a joint analysis of the SDSS-II and SNLS supernova samples," *A&A*, vol. 568, p. A22, Aug. 2014.

[4] I. P. Pskovskii, "Light curves, color curves, and expansion velocity of type I supernovae as functions of the rate of brightness decline," *Soviet Ast.*, vol. 21, pp. 675–682, Dec. 1977.

[5] Y. P. Pskovskii, "Photometric classification and basic parameters of type I supernovae," *Soviet Ast.*, vol. 28, pp. 658–664, Dec. 1984.

[6] B. W. Rust, *Use of supernovae light curves for testing the expansion hypothesis and other cosmological relations*. PhD thesis, Oak Ridge National Lab., TN., 1974.

[7] M. Hamuy, M. M. Phillips, N. B. Suntzeff, R. A. Schommer, J. Maza, and R. Aviles, "The Hubble Diagram of the Calan/Tololo Type IA Supernovae and the Value of HO," *AJ*, vol. 112, p. 2398, Dec. 1996.

[8] R. Tripp, "A two-parameter luminosity correction for Type IA supernovae," *A&A*, vol. 331, pp. 815–820, Mar. 1998.

[9] M. M. Phillips, "The absolute magnitudes of Type IA supernovae," *ApJL*, vol. 413, pp. L105–L108, Aug. 1993.

[10] M. M. Phillips, P. Lira, N. B. Suntzeff, R. A. Schommer, M. Hamuy, and J. Maza, "The Reddening-Free Decline Rate Versus Luminosity

Relationship for Type IA Supernovae," *AJ*, vol. 118, pp. 1766–1776, Oct. 1999.

[11] S. Perlmutter, S. Gabi, G. Goldhaber, A. Goobar, D. E. Groom, I. M. Hook, A. G. Kim, M. Y. Kim, J. C. Lee, R. Pain, C. R. Pennypacker, I. A. Small, R. S. Ellis, R. G. McMahon, B. J. Boyle, P. S. Bunclark, D. Carter, M. J. Irwin, K. Glazebrook, H. J. M. Newberg, A. V. Filippenko, T. Matheson, M. Dopita, and W. J. Couch, "Measurements of the Cosmological Parameters Ω and Λ from the First Seven Supernovae at z <= 0.35," *ApJ*, vol. 483, pp. 565–581, July 1997.

[12] A. Riess, W. Press, and R. Kirshner, "A precise distance indicator: Type ia supernova multicolor light curve shapes," *AJ*, vol. 473, p. 88, 1996.

[13] S. Jha, A. G. Riess, and R. P. Kirshner, "Improved Distances to Type Ia Supernovae with Multicolor Light-Curve Shapes: MLCS2k2," *ApJ*, vol. 659, pp. 122–148, Apr. 2007.

[14] J. L. Prieto, A. Rest, and N. B. Suntzeff, "A New Method to Calibrate the Magnitudes of Type Ia Supernovae at Maximum Light," *ApJ*, vol. 647, pp. 501–512, Aug. 2006.

[15] J. Guy, P. Astier, S. Nobili, N. Regnault, and R. Pain, "SALT: a spectral adaptive light curve template for type Ia supernovae," *A&A*, vol. 443, pp. 781–791, Dec. 2005.

[16] J. Guy, P. Astier, S. Baumont, D. Hardin, R. Pain, N. Regnault, S. Basa, R. G. Carlberg, A. Conley, S. Fabbro, D. Fouchez, I. M. Hook, D. A. Howell, K. Perrett, C. J. Pritchet, J. Rich, M. Sullivan, P. Antilogus, E. Aubourg, G. Bazin, J. Bronder, M. Filiol, N. Palanque-Delabrouille, P. Ripoche, and V. Ruhlmann-Kleider, "SALT2: using distant supernovae to improve the use of type Ia supernovae as distance indicators," *A&A*, vol. 466, pp. 11–21, Apr. 2007.

[17] L. Wang, G. Goldhaber, G. Aldering, and S. Perlmutter, "Multicolor Light Curves of Type Ia Supernovae on the Color-Magnitude Diagram: A Novel Step toward More Precise Distance and Extinction Estimates," *ApJ*, vol. 590, pp. 944–970, June 2003.

[18] J. Whelan and I. Iben, Jr., "Binaries and Supernovae of Type I," *ApJ*, vol. 186, pp. 1007–1014, Dec. 1973.

[19] I. Iben, Jr. and A. V. Tutukov, "Supernovae of type I as end products of the evolution of binaries with components of moderate initial mass (M not greater than about 9 solar masses)," *ApJS*, vol. 54, pp. 335–372, Feb. 1984.

[20] R. F. Webbink, "Double white dwarfs as progenitors of R Coronae Borealis stars and Type I supernovae," *ApJ*, vol. 277, pp. 355–360, Feb. 1984.

[21] A. N. Aguirre, "Dust versus Cosmic Acceleration," *ApJL*, vol. 512, pp. L19–L22, Feb. 1999.

[22] A. I. Bogomazov and A. V. Tutukov, "Type Ia supernovae: Nonstandard candles of the universe," *Astronomy Reports*, vol. 55, pp. 497–504, June 2011.

[23] M. V. Pruzhinskaya, E. S. Gorbovskoy, and V. M. Lipunov, ""Pure" supernovae and accelerated expansion of the Universe," *Astronomy Letters*, vol. 37, pp. 663–669, Oct. 2011.

[24] M. Sullivan, R. S. Ellis, G. Aldering, R. Amanullah, P. Astier, G. Blanc, M. S. Burns, A. Conley, S. E. Deustua, M. Doi, S. Fabbro, G. Folatelli, A. S. Fruchter, G. Garavini, R. Gibbons, G. Goldhaber, A. Goobar, D. E. Groom, D. Hardin, I. Hook, D. A. Howell, M. Irwin, A. G. Kim, R. A. Knop, C. Lidman, R. McMahon, J. Mendez, S. Nobili, P. E. Nugent, R. Pain, N. Panagia, C. R. Pennypacker, S. Perlmutter, R. Quimby, J. Raux, N. Regnault, P. Ruiz-Lapuente, B. Schaefer, K. Schahmaneche, A. L. Spadafora, N. A. Walton, L. Wang, W. M. Wood-Vasey, and N. Yasuda, "The Hubble diagram of type Ia supernovae as a function of host galaxy morphology," *MNRAS*, vol. 340, pp. 1057–1075, Apr. 2003.

[25] V. M. Lipunov, I. E. Panchenko, and M. V. Pruzhinskaya, "The mechanism of supernova Ia explosion in elliptical galaxies," *New A*, vol. 16, pp. 250–252, July 2011.

[26] E. P. Hubble, "Extragalactic nebulae.," *ApJ*, vol. 64, Dec. 1926.

[27] E. P. Hubble, *Realm of the Nebulae*. 1936.

[28] G. de Vaucouleurs, "Classification and Morphology of External Galaxies.," *Handbuch der Physik*, vol. 53, p. 275, 1959.

[29] A. Sandage, *The Hubble atlas of galaxies*. 1961.

[30] R. J. Buta, *Galaxy Morphology*, p. 1. 2013.

[31] D. Hunter, "Star Formation in Irregular Galaxies: A Review of Several Key Questions," *PASP*, vol. 109, pp. 937–950, Sept. 1997.

[32] A. Baillard, E. Bertin, V. de Lapparent, P. Fouqué, S. Arnouts, Y. Mellier, R. Pelló, J.-F. Leborgne, P. Prugniel, D. Makarov, L. Makarova, H. J. McCracken, A. Bijaoui, and L. Tasca, "The EFIGI catalogue of 4458 nearby galaxies with detailed morphology," *A&A*, vol. 532, p. A74, Aug. 2011.

[33] B. Reindl, G. A. Tammann, A. Sandage, and A. Saha, "Reddening, Absorption, and Decline Rate Corrections for a Complete Sample of Type Ia Supernovae Leading to a Fully Corrected Hubble Diagram to v $< 30{,}000$ km s^{-1}," *ApJ*, vol. 624, pp. 532–554, May 2005.

[34] J. D. Neill, M. Sullivan, D. A. Howell, A. Conley, M. Seibert, D. C. Martin, T. A. Barlow, K. Foster, P. G. Friedman, P. Morrissey, S. G. Neff, D. Schiminovich, T. K. Wyder, L. Bianchi, J. Donas, T. M. Heckman, Y.-W. Lee, B. F. Madore, B. Milliard, R. M. Rich, and A. S. Szalay, "The Local Hosts of Type Ia Supernovae," *ApJ*, vol. 707, pp. 1449–1465, Dec. 2009.

[35] C. Zheng, R. W. Romani, M. Sako, J. Marriner, B. Bassett, A. Becker, C. Choi, D. Cinabro, F. DeJongh, D. L. Depoy, B. Dilday, M. Doi, J. A. Frieman, P. M. Garnavich, C. J. Hogan, J. Holtzman, M. Im, S. Jha, R. Kessler, K. Konishi, H. Lampeitl, J. L. Marshall, D. McGinnis, G. Miknaitis, R. C. Nichol, J. L. Prieto, A. G. Riess, M. W. Richmond, D. P. Schneider, M. Smith, N. Takanashi, K. Tokita, K. van der Heyden, N. Yasuda, R. J. Assef, J. Barentine, R. Bender, R. D. Blandford, M. Bremer, H. Brewington, C. A. Collins, A. Crotts, J. Dembicky, J. Eastman, A. Edge, E. Elson, M. E. Eyler, A. V. Filippenko, R. J. Foley, S. Frank, A. Goobar, M. Harvanek, U. Hopp, Y. Ihara, S. Kahn, W. Ketzeback, S. J. Kleinman, W. Kollatschny, J. Krzesiński, G. Leloudas, D. C. Long, J. Lucey, E. Malanushenko, V. Malanushenko,

R. J. McMillan, C. W. Morgan, T. Morokuma, A. Nitta, L. Ostman, K. Pan, A. K. Romer, G. Saurage, K. Schlesinger, S. A. Snedden, J. Sollerman, M. Stritzinger, L. C. Watson, S. Watters, J. C. Wheeler, and D. York, "First-Year Spectroscopy for the Sloan Digital Sky Survey-II Supernova Survey," *AJ*, vol. 135, pp. 1766–1784, May 2008.

[36] R. B. Tully, H. M. Courtois, A. E. Dolphin, J. R. Fisher, P. Héraudeau, B. A. Jacobs, I. D. Karachentsev, D. Makarov, L. Makarova, S. Mitronova, L. Rizzi, E. J. Shaya, J. G. Sorce, and P.-F. Wu, "Cosmicflows-2: The Data," *AJ*, vol. 146, p. 86, Oct. 2013.

[37] R. Chary, M. E. Dickinson, H. I. Teplitz, A. Pope, and S. Ravindranath, "Dust in the Host Galaxies of Supernovae," *ApJ*, vol. 635, pp. 1022–1030, Dec. 2005.

[38] J. Meyers, G. Aldering, K. Barbary, L. F. Barrientos, M. Brodwin, K. S. Dawson, S. Deustua, M. Doi, P. Eisenhardt, L. Faccioli, H. K. Fakhouri, A. S. Fruchter, D. G. Gilbank, M. D. Gladders, G. Goldhaber, A. H. Gonzalez, T. Hattori, E. Hsiao, Y. Ihara, N. Kashikawa, B. Koester, K. Konishi, C. Lidman, L. Lubin, T. Morokuma, T. Oda, S. Perlmutter, M. Postman, P. Ripoche, P. Rosati, D. Rubin, E. Rykoff, A. Spadafora, S. A. Stanford, N. Suzuki, N. Takanashi, K. Tokita, N. Yasuda, and T. Supernova Cosmology Project, "The Hubble Space Telescope Cluster Supernova Survey. III. Correlated Properties of Type Ia Supernovae and Their Hosts at $0.9 < \mathrm{Z} < 1.46$," *ApJ*, vol. 750, p. 1, May 2012.

[39] J. Marriner, J. P. Bernstein, R. Kessler, H. Lampeitl, R. Miquel, J. Mosher, R. C. Nichol, M. Sako, D. P. Schneider, and M. Smith, "A More General Model for the Intrinsic Scatter in Type Ia Supernova Distance Moduli," *ApJ*, vol. 740, p. 72, Oct. 2011.

[40] M. Hamuy, M. M. Phillips, J. Maza, N. B. Suntzeff, R. A. Schommer, and R. Aviles, "A Hubble diagram of distant type IA supernovae," *AJ*, vol. 109, pp. 1–13, Jan. 1995.

[41] A. G. Riess, R. P. Kirshner, B. P. Schmidt, S. Jha, P. Challis, P. M. Garnavich, A. A. Esin, C. Carpenter, R. Grashius, R. E. Schild, P. L. Berlind, J. P. Huchra, C. F. Prosser, E. E. Falco, P. J. Benson, C. Briceño, W. R. Brown, N. Caldwell, I. P. dell'Antonio, A. V. Filippenko, A. A. Goodman, N. A. Grogin, T. Groner, J. P. Hughes, P. J.

Green, R. A. Jansen, J. T. Kleyna, J. X. Luu, L. M. Macri, B. A. McLeod, K. K. McLeod, B. R. McNamara, B. McLean, A. A. E. Milone, J. J. Mohr, D. Moraru, C. Peng, J. Peters, A. H. Prestwich, K. Z. Stanek, A. Szentgyorgyi, and P. Zhao, "BVRI Light Curves for 22 Type IA Supernovae," *AJ*, vol. 117, pp. 707–724, Feb. 1999.

[42] M. Hamuy, S. C. Trager, P. A. Pinto, M. M. Phillips, R. A. Schommer, V. Ivanov, and N. B. Suntzeff, "A Search for Environmental Effects on Type IA Supernovae," *AJ*, vol. 120, pp. 1479–1486, Sept. 2000.

[43] M. Sullivan, D. Le Borgne, C. J. Pritchet, A. Hodsman, J. D. Neill, D. A. Howell, R. G. Carlberg, P. Astier, E. Aubourg, D. Balam, S. Basa, A. Conley, S. Fabbro, D. Fouchez, J. Guy, I. Hook, R. Pain, N. Palanque-Delabrouille, K. Perrett, N. Regnault, J. Rich, R. Taillet, S. Baumont, J. Bronder, R. S. Ellis, M. Filiol, V. Lusset, S. Perlmutter, P. Ripoche, and C. Tao, "Rates and Properties of Type Ia Supernovae as a Function of Mass and Star Formation in Their Host Galaxies," *ApJ*, vol. 648, pp. 868–883, Sept. 2006.

[44] M. Sullivan, A. Conley, D. A. Howell, J. D. Neill, P. Astier, C. Balland, S. Basa, R. G. Carlberg, D. Fouchez, J. Guy, D. Hardin, I. M. Hook, R. Pain, N. Palanque-Delabrouille, K. M. Perrett, C. J. Pritchet, N. Regnault, J. Rich, V. Ruhlmann-Kleider, S. Baumont, E. Hsiao, T. Kronborg, C. Lidman, S. Perlmutter, and E. S. Walker, "The dependence of Type Ia Supernovae luminosities on their host galaxies," *MNRAS*, vol. 406, pp. 782–802, Aug. 2010.

[45] M. Smith, R. C. Nichol, B. Dilday, J. Marriner, R. Kessler, B. Bassett, D. Cinabro, J. Frieman, P. Garnavich, S. W. Jha, H. Lampeitl, M. Sako, D. P. Schneider, and J. Sollerman, "The SDSS-II Supernova Survey: Parameterizing the Type Ia Supernova Rate as a Function of Host Galaxy Properties," *ApJ*, vol. 755, p. 61, Aug. 2012.

[46] J. Johansson, D. Thomas, J. Pforr, C. Maraston, R. C. Nichol, M. Smith, H. Lampeitl, A. Beifiori, R. R. Gupta, and D. P. Schneider, "SN Ia host galaxy properties from Sloan Digital Sky Survey-II spectroscopy," *MNRAS*, vol. 435, pp. 1680–1700, Oct. 2013.

[47] M. Hicken, W. M. Wood-Vasey, S. Blondin, P. Challis, S. Jha, P. L. Kelly, A. Rest, and R. P. Kirshner, "Improved Dark Energy Constraints

from ˜100 New CfA Supernova Type Ia Light Curves," *ApJ*, vol. 700, pp. 1097–1140, Aug. 2009.

[48] M. Rigault, Y. Copin, G. Aldering, P. Antilogus, C. Aragon, S. Bailey, C. Baltay, S. Bongard, C. Buton, A. Canto, F. Cellier-Holzem, M. Childress, N. Chotard, H. K. Fakhouri, U. Feindt, M. Fleury, E. Gangler, P. Greskovic, J. Guy, A. G. Kim, M. Kowalski, S. Lombardo, J. Nordin, P. Nugent, R. Pain, E. Pécontal, R. Pereira, S. Perlmutter, D. Rabinowitz, K. Runge, C. Saunders, R. Scalzo, G. Smadja, C. Tao, R. C. Thomas, and B. A. Weaver, "Evidence of environmental dependencies of Type Ia supernovae from the Nearby Supernova Factory indicated by local Hα," *A&A*, vol. 560, p. A66, Dec. 2013.

[49] H. Aihara, C. Allende Prieto, D. An, S. F. Anderson, É. Aubourg, E. Balbinot, T. C. Beers, A. A. Berlind, S. J. Bickerton, D. Bizyaev, M. R. Blanton, J. J. Bochanski, A. S. Bolton, J. Bovy, W. N. Brandt, J. Brinkmann, P. J. Brown, J. R. Brownstein, N. G. Busca, H. Campbell, M. A. Carr, Y. Chen, C. Chiappini, J. Comparat, N. Connolly, M. Cortes, R. A. C. Croft, A. J. Cuesta, L. N. da Costa, J. R. A. Davenport, K. Dawson, S. Dhital, A. Ealet, G. L. Ebelke, E. M. Edmondson, D. J. Eisenstein, S. Escoffier, M. Esposito, M. L. Evans, X. Fan, B. Femenía Castellá, A. Font-Ribera, P. M. Frinchaboy, J. Ge, B. A. Gillespie, G. Gilmore, J. I. González Hernández, J. R. Gott, A. Gould, E. K. Grebel, J. E. Gunn, J.-C. Hamilton, P. Harding, D. W. Harris, S. L. Hawley, F. R. Hearty, S. Ho, D. W. Hogg, J. A. Holtzman, K. Honscheid, N. Inada, I. I. Ivans, L. Jiang, J. A. Johnson, C. Jordan, W. P. Jordan, E. A. Kazin, D. Kirkby, M. A. Klaene, G. R. Knapp, J.-P. Kneib, C. S. Kochanek, L. Koesterke, J. A. Kollmeier, R. G. Kron, H. Lampeitl, D. Lang, J.-M. Le Goff, Y. S. Lee, Y.-T. Lin, D. C. Long, C. P. Loomis, S. Lucatello, B. Lundgren, R. H. Lupton, Z. Ma, N. MacDonald, S. Mahadevan, M. A. G. Maia, M. Makler, E. Malanushenko, V. Malanushenko, R. Mandelbaum, C. Maraston, D. Margala, K. L. Masters, C. K. McBride, P. M. McGehee, I. D. McGreer, B. Ménard, J. Miralda-Escudé, H. L. Morrison, F. Mullally, D. Muna, J. A. Munn, H. Murayama, A. D. Myers, T. Naugle, A. F. Neto, D. C. Nguyen, R. C. Nichol, R. W. O'Connell, R. L. C. Ogando, M. D. Olmstead, D. J. Oravetz, N. Padmanabhan, N. Palanque-Delabrouille, K. Pan, P. Pandey, I. Pâris, W. J. Percival, P. Petitjean, R. Pfaffenberger,

J. Pforr, S. Phleps, C. Pichon, M. M. Pieri, F. Prada, A. M. Price-Whelan, M. J. Raddick, B. H. F. Ramos, C. Reylé, J. Rich, G. T. Richards, H.-W. Rix, A. C. Robin, H. J. Rocha-Pinto, C. M. Rockosi, N. A. Roe, E. Rollinde, A. J. Ross, N. P. Ross, B. M. Rossetto, A. G. Sánchez, C. Sayres, D. J. Schlegel, K. J. Schlesinger, S. J. Schmidt, D. P. Schneider, E. Sheldon, Y. Shu, J. Simmerer, A. E. Simmons, T. Sivarani, S. A. Snedden, J. S. Sobeck, M. Steinmetz, M. A. Strauss, A. S. Szalay, M. Tanaka, A. R. Thakar, D. Thomas, J. L. Tinker, B. M. Tofflemire, R. Tojeiro, C. A. Tremonti, J. Vandenberg, M. Vargas Magaña, L. Verde, N. P. Vogt, D. A. Wake, J. Wang, B. A. Weaver, D. H. Weinberg, M. White, S. D. M. White, B. Yanny, N. Yasuda, C. Yeche, and I. Zehavi, "The Eighth Data Release of the Sloan Digital Sky Survey: First Data from SDSS-III," *ApJS*, vol. 193, p. 29, Apr. 2011.

Appendix

Table 6: Final sample of SN Ia used in current analysis. Host types are divided by three categories: elliptical/lenticular (E/L), early-type spiral (ES), and late-type spiral (LS). For SDSS galaxies the name is IDobj taken from SDSS Data Release 8 [49].

SN name	Host name	$z_{\rm cmb}$	Host type
sn1999ac	NGC6063	0.01006	LS
sn1997do	UGC3845	0.01055	ES
sn2002dp	NGC7678	0.010888	LS
sn2006bh	NGC7329	0.011184	ES
sn2005al	NGC5304	0.012317	E/L
sn2001ep	NGC1699	0.013324	LS
sn1999dq	NGC976	0.013533	LS
sn2002ha	NGC6962	0.013652	ES
sn2001bt	IC4830	0.014151	ES
sn1997e	NGC2258	0.014256	E/L
sn1992al	ESO234-69	0.014411	ES
sn1999dk	UGC1087	0.01444	LS
sn2005bo	NGC4708	0.014467	ES
sn2001fe	UGC5129	0.014575	LS
sn2006n	MCG+11-08-012	0.0147	E/L
sn2005kc	NGC7311	0.01496	ES
sn2005el	NGC1819	0.015154	ES
sn2004eo	NGC6928	0.015469	ES
sn2001cn	IC4758	0.015487	LS
sn2001bf	2MASXJ18013361+2615109	0.015504	E/L
sn2001cz	NGC4679	0.015554	LS
sn1999aa	NGC2595	0.015573	ES
sn1994s	NGC4495	0.015664	ES
sn2004ey	UGC11816	0.015678	ES
sn2001v	NGC3987	0.015791	ES
sn1996bv	UGC3432	0.016966	LS
sn2006ax	NGC3663	0.017387	ES
sn1998v	NGC6627	0.01745	ES
sn2000dk	NGC382	0.017483	E/L

sn1998ef	UGC646	0.017672	ES
sn2007ci	NGC3873	0.018599	E/L
sn1992bo	ESO352-57	0.018902	E/L
sn2005ki	NGC3332	0.020396	E/L
sn1992bc	ESO300-9	0.020792	ES
sn2003w	UGC5234	0.020997	LS
sn2002jy	NGC477	0.021541	LS
sn2007bc	UGC6332	0.021706	ES
sn2006bq	NGC6685	0.021956	E/L
sn2008bf	NGC4055	0.022068	E/L
sn1995ak	IC1844	0.022399	LS
sn2006et	NGC232	0.022466	ES
sn2006ar	MCG+11-13-036	0.02298	ES
sn2006cp	UGC7357	0.023321	LS
sn2000ca	2MASXJ13352270-3409338	0.02336	LS
sn2006ac	NGC4619	0.023471	ES
sn2000cn	UGC11064	0.023552	ES
sn2007f	UGC8162	0.02381	LS
sn1993h	ESO445-066	0.023909	ES
sn2006sr	UGC14	0.024159	LS
sn2005bg	MCG+03-31-093	0.024586	ES
sn2002he	UGC4322	0.024725	E/L
sn2002bf	2MASXJ10154226+5540030	0.024746	ES
sn1994m	NGC4493	0.024951	E/L
sn1992ag	ESO508-67	0.025198	LS
sn2005ms	UGC04614	0.026567	LS
sn1999gp	UGC01993	0.026677	ES
sn2005na	UGC3634	0.026881	ES
sn2007co	MCG+05-43-016	0.027064	LS
sn2004gs	MCG+03-22-020	0.027499	E/L
sn1992p	IC3690	0.027637	ES
sn1998ab	NGC4704	0.027688	ES
sn2002de	NGC6104	0.027748	ES
sn2003u	NGC6365A	0.028561	LS
sn2005eq	MCG-01-09-006	0.029086	LS
sn2006qo	UGC4133	0.029526	LS
sn1990o	MCG+03-44-003	0.030325	ES
sn2001ba	2MASXJ11380048-3219286	0.030381	ES

sn2003ch	2MASXJ07175757+0941218	0.030416	E/L
sn1997dg	SDSSJ234014.21+261211.8	0.030482	ES
sn1996c	MCG+08-25-047	0.030721	ES
sn2006bt	MCG+03-41-004	0.031484	ES
sn2006az	NGC4172	0.031485	ES
sn2007bd	UGC4455	0.031638	ES
sn1999cc	NGC6038	0.031764	LS
sn2004as	SDSSJ112538.81+224952.2	0.032538	LS
sn2004l	MCG+03-27-038	0.033173	ES
sn2006s	UGC7934	0.033255	ES
sn2006gr	UGC12071	0.033614	ES
sn2005iq	MCG-03-01-008	0.034074	ES
sn1996bl	2MASXJ00361813+1123354	0.034854	ES
sn2003iv	2MASXJ02500884+1250372	0.034971	E/L
sn1992bg	2MASXJ07415700-6231144	0.035218	ES
sn2002hd	2MASXJ08540470-0710597	0.035755	E/L
sn2000cf	2MASXJ15525577+6556079	0.036934	ES
sn2006mo	MCG+06-02-017	0.036969	ES
sn2001eh	UGC1162	0.037075	ES
sn2002hu	2MASXJ02181834+3727513	0.038086	ES
sn1999aw	SCPJ110136.37-060631.6	0.039083	LS
sn2001az	UGC10483	0.040259	ES
sn2005lz	UGC1666	0.040689	ES
sn1992bh	LSBG-F119-024	0.041657	ES
sn1992bl	ESO291-11	0.0424	ES
sn2005hc	MCG+00-06-003	0.04492	ES
sn2004gu	2MASXJ12462478+1156577	0.046856	ES
sn1995ac	2MASXJ22453410-0845026	0.048984	ES
sn1993ag	2MASXJ10033546-3527410	0.049325	E/L
sn1990af	2MASXJ21345926-6244143	0.049519	E/L
sn1993o	2MASXJ13310895-3312576	0.053126	E/L
sn1998dx	UGC11149	0.05386	E/L
sn2006ob	UGC1333	0.059289	ES
sn1992bs	2MASXJ03292797-3716222	0.063345	LS
sn2006an	SDSSJ121438.73+121347.7	0.065193	LS
sn2006on	SDSSJ215558.49-010413.0	0.069751	E/L
sn1993b	PGC662260	0.070153	ES
sn1992ae	[WM92]212426.8-614612	0.074579	E/L

sn2005ir	PGC3116670	0.07487	ES
sn1999bp	PGC998264	0.078317	ES
sn1992bp	2MASXJ03363839-1821123	0.07884	E/L
sn2005ag	2MASXJ14564322+0919361	0.080103	ES
SDSS10805	1237666407898940000	0.04413	LS
SDSS14279	1237666339726690000	0.04428	ES
SDSS3901	1237663784203910000	0.062818	LS
SDSS10028	1237666339726360000	0.064229	E/L
SDSS6057	1237666299482800000	0.06651	LS
SDSS12781	1237657189833840000	0.08304	E/L
SDSS722	1237657191979290000	0.08522	E/L
SDSS3592	1237663204922490000	0.08528	ES
SDSS21502	1237656906352300000	0.08784	E/L
SDSS774	1237657069547680000	0.09243	ES
SDSS2102	1237656568648830000	0.09401	LS
SDSS21034	1237678617430130000	0.10751	ES
SDSS7147	1237657190900830000	0.10924	E/L
SDSS5395	1237663784219120000	0.11635	LS
SDSS8719	1237663783127020000	0.11651	LS
SDSS2561	1237678437019290000	0.11741	ES
SDSS19953	1237663479795480000	0.11767	E/L
SDSS2916	1237678617398540000	0.12303	ES
SDSS6406	1237660024523920000	0.12376	ES
SDSS2992	1237663237667550000	0.12608	ES
SDSS744	1237663543682530000	0.12649	LS
SDSS1032	1237666302164660000	0.12903	ES
SDSS5751	1237663204919280000	0.12953	ES
SDSS1794	1237663542603810000	0.14139	LS
SDSS2635	1237663237129500000	0.1431	LS
SDSS8921	1237663543143830000	0.14401	LS
SDSS11300	1237657190371300000	0.14547	LS
SDSS2031	1237656567038150000	0.15186	LS
SDSS5550	1237657191443660000	0.15473	ES
SDSS3317	1237657071695820000	0.15999	LS
SDSS3087	1237666338116930000	0.1644	LS
SDSS12843	1237657189815680000	0.16565	E/L
SDSS12856	1237663544220980000	0.17028	E/L
SDSS3080	1237666338115360000	0.17374	ES

SDSS5635	1237663543147360000	0.1781	LS
SDSS2372	1237657070091110000	0.17962	E/L
SDSS6936	1237656567579870000	0.17969	LS
SDSS17215	1237666302168200000	0.18079	ES
SDSS8213	1237656906354000000	0.18327	ES
SDSS6304	1237678617429410000	0.18965	LS
SDSS762	1237666338114770000	0.1901	ES
SDSS2246	1237666299481750000	0.19422	LS
SDSS15222	1237657191980200000	0.19801	E/L
SDSS7243	1237663479793390000	0.20231	LS
SDSS7847	1237666407919780000	0.21134	ES
SDSS2330	1237678434328180000	0.21179	ES
SDSS8495	1237656567585180000	0.21295	ES
SDSS9467	1237678595929410000	0.21698	ES
SDSS5533	1237663543682270000	0.21829	LS
SDSS3452	1237663544221760000	0.22893	LS
SDSS3377	1237666302167880000	0.24448	LS
SDSS3451	1237663544221500000	0.24851	ES
SDSS3199		0.24961	ES
SDSS5717	1237666339189560000	0.25037	LS
SDSS9032	1237663542612590000	0.25249	LS
SDSS9457	1237663543685420000	0.25539	ES
SDSS1112	1237663478724430000	0.25611	ES
SDSS17340	1237666408460450000	0.25617	E/L
SDSS6108	1237663543696750000	0.258	LS
SDSS8046	1237663784751400000	0.25833	E/L
SDSS2017	1237663479793710000	0.26014	ES
SDSS1253	1237663457779380000	0.26059	ES
SDSS2422	1237657191979810000	0.26349	LS
SDSS2943		0.26405	LS
SDSS6315	1237659743703800000	0.26576	LS
SDSS6192	1237678617412760000	0.27044	LS
SDSS4046	1237657191976530000	0.27544	E/L
SDSS4000	1237663783674120000	0.27745	LS
SDSS5957	1237663783675760000	0.27852	LS
SDSS6196	1237663542612460000	0.27916	E/L
SDSS6249	1237657190369790000	0.29287	LS
SDSS6137		0.29888	ES

SDSS5391	1237663237129310000	0.30021	LS
SDSS6699	1237656567042800000	0.30915	ES
SDSS5844		0.30929	LS
SDSS16211	1237666408437250000	0.30933	E/L
SDSS7475		0.32045	LS
SDSS4241	1237657189836850000	0.33051	LS
SDSS4679	1237663204923610000	0.33103	LS
SDSS2533	1237663783674180000	0.3388	E/L
SDSS4577	1237666408459270000	0.36193	ES
SDSS7779	1237663543137270000	0.37986	LS
SDSS11206	1237657192517270000	0.38026	ES